PROCEEDINGS OF SCIENCE

First Measurements of Neutrino Interaction Cross Sections with FASER

Yuxiao Wang[a,*] on behalf of the FASER collaboration

[a] *Tsinghua University, Beijing, China*

E-mail: yuxiao.wang@cern.ch, yuxiao.phys@gmail.com

The FASER experiment at the LHC is designed to search for light, weakly-coupled new particles, and to study high-energy neutrinos. The experiment has been running since 2022, and has collected nearly 200/fb of pp collision data. FASER has released several neutrino results including the first observation of electron and muon neutrinos at a particle collider, the first measurement of the muon and electron neutrino interaction cross sections in the TeV energy range, and the first differential measurement with muon neutrinos and anti-neutrinos. This talk will summarise the FASER experiment, the neutrino results, and discuss future prospects for FASER neutrino results.

Presented at the 32nd International Symposium on Lepton Photon Interactions at High Energies, Madison, Wisconsin, USA, August 25-29, 2025

[*] Speaker

ISSN 1824-8039. Published by SISSA Medialab. https://pos.sissa.it/

1. Introduction

The FASER experiment is located in the TI12 tunnel, 480 meters downstream from the ATLAS interaction point at the Large Hadron Collider (LHC). This unique forward geometry allows FASER to detect particles produced at very small angles that escape detection by the main LHC experiments. The experiment has two primary physics goals: searching for new light, long-lived particles and detecting TeV-scale neutrinos produced in proton-proton collisions [1].

FASER comprises both an electronic detector and the FASERν emulsion detector [2]. The FASERν detector consists of 730 layers of 1.1 mm tungsten plates interleaved with emulsion films, providing exceptional spatial resolution of approximately 0.3 μm. This detector has a target mass of 314.7 kg (currently analyzed volume) and dimensions of 25×30 cm^2 with a total length of 1.1 m and total weight of 1.1 t. The emulsion films, produced in Japan using silver bromide crystals, are exchanged approximately three times per year.

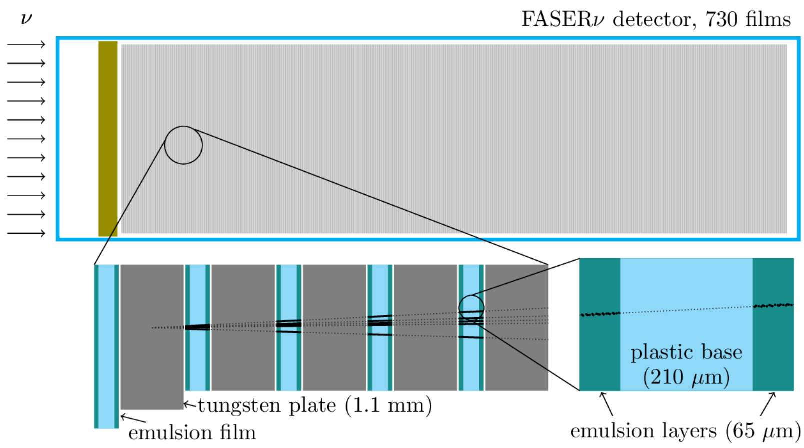

Figure 1: A schematic illustration of the FASERν emulsion detector.

The neutrinos detected by FASER originate primarily from the decay of light hadrons (π, K) and charm mesons (D) produced in the very forward direction ($\eta > 8.5$) of LHC collisions. At 13.6 TeV center-of-mass energy, FASER expects approximately 1,700 ν_e interactions, 8,500 ν_μ interactions, and 30 ν_τ interactions per 250 fb^{-1} of integrated luminosity during Run 3 [3].

FASER has achieved several historic milestones including the first observation of neutrinos at a particle collider [4], the first detection of ν_e and ν_μ at the LHC [5], and the first neutrino cross-section measurements in the TeV energy range. This proceeding focuses on the latest cross-section measurements.

2. Detector Performance and Event Selection

2.1 Detector Capabilities

The FASERν emulsion detector provides exceptional tracking capabilities with 0.3 μm position resolution, corresponding to approximately 0.04 mrad angular resolution for a 1 cm track. Performance validation was conducted using 2024 testbeam data at the CERN SPS H8 beamline, demonstrating ~20% energy resolution at 200 GeV [6].

Momentum measurements for muons utilize multiple Coulomb scattering (MCS), achieving $\Delta p/p \approx 0.30$ at 200 GeV with good linearity extending beyond 1 TeV. Electromagnetic shower energy reconstruction uses segment multiplicity in the core of the EM shower, achieving $\Delta E/E \approx 0.21$ at 200 GeV with linear response from 100 GeV to 2 TeV.

2.2 Event Selection

Neutrino events are identified through charged-current (CC) interactions producing a primary lepton and hadronic shower. The selection criteria require vertex reconstruction with $N_{\text{charged}} \geq 5$ tracks and $N_{\tan\theta \leq 0.1} \geq 4$ tracks in the forward cone. For ν_e CC events, we require an electron track with $E > 200$ GeV, while ν_μ CC events require a long track with $p > 200$ GeV extending through more than 100 films. Additionally, the angular separation $\Delta\phi > 90$ between lepton and hadronic system is required, along with lepton angle $\tan\theta_{\text{lep}} > 0.005$.

The primary background comes from neutral hadron interactions, primarily K_L^0 decays. Background levels were estimated to be $0.06^{+0.04}_{-0.02}$ for ν_e CC and $0.54^{+0.22}_{-0.17}$ for ν_μ CC.

3. Data and Simulations

The analysis uses 9.5 fb^{-1} of LHC Run 3 data collected during 2022, corresponding to a target mass of 314.7 kg (Zone 3 and 4, comprising 620 emulsion plates). This represents approximately 1.7% of the full Run 3 dataset expected by 2025.

Monte Carlo simulations employ multiple hadron production models for light hadron production (EPOS-LHC, QGSJET II-04, SIBYLL 2.3d, and PYTHIA 8) and charm hadron production (POWHEG+PYTHIA 8).

The neutrino flux is dominated by ν_μ and $\bar{\nu}_\mu$ from light hadron decays, with a subdominant component from charm decays contributing primarily to ν_e and ν_μ at higher energies. The peak flux occurs around 600-1000 GeV, with significant contributions extending beyond 2 TeV.

4. Results

4.1 Electron Neutrino Cross Sections

The analysis observed 5 ν_e CC candidate events with an expected background of $0.06^{+0.04}_{-0.02}$, corresponding to a significance of 5.2σ. The highest energy electron neutrino observed had $E_e = 1.5$ TeV, representing the highest energy neutrino measured with flavor identification to date.

Electron identification relies on the characteristic electromagnetic shower topology in the emulsion-tungsten sandwich structure. When an electron interacts with the tungsten plates, it initiates an electromagnetic cascade through bremsstrahlung and pair production processes. The shower develops over multiple layers, creating a distinctive pattern of high-multiplicity track segments in the emulsion films. The electron energy is reconstructed using the segment multiplicity method, which counts the number of charged particles (track segments) in the shower core within a defined cone around the shower axis. This technique exploits the approximately logarithmic relationship between shower multiplicity and primary electron energy. The method achieves energy resolution of $\Delta E/E \approx 0.21$ at 200 GeV, improving to approximately 20% at 2 TeV. The electromagnetic shower is distinguished from hadronic showers by its more compact transverse profile, higher track density in the core region, and characteristic longitudinal development matching Molière radius expectations.

This measurement is consistent with Standard Model predictions from the Bodek-Yang model within uncertainties. The dominant systematic uncertainty ($^{+70}_{-22}\%$) arises from neutrino flux predictions, followed by reconstruction efficiency (20%) and hadronization modeling ($^{+22}_{-5}\%$).

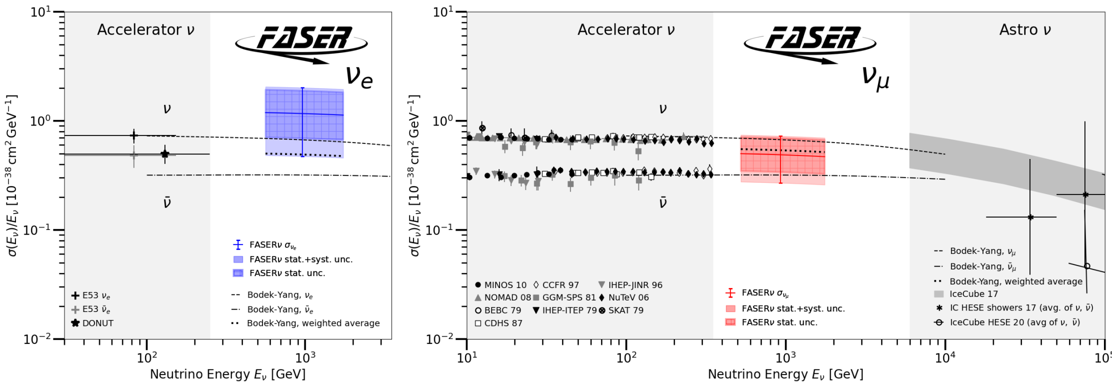

Figure 2: The measured cross section per nucleon for ν_e (left) and ν_μ (right). The dashed contours labelled "Bodek-Yang" are cross sections predicted by the Bodek-Yang model, as implemented in GENIE.

4.2 Muon Neutrino Cross Sections

The analysis observed 20 ν_μ CC candidate events with an expected background of $0.54^{+0.22}_{-0.17}$, corresponding to a significance of 5.7σ. The muon momentum measurements extended up to several hundred GeV, with excellent agreement between reconstructed and true momenta.

Muon identification exploits the characteristic signature of minimum ionizing particles traversing the detector. Unlike electrons that shower rapidly, muons penetrate through many tungsten plates while maintaining a nearly straight trajectory, leaving isolated track segments in consecutive emulsion layers. Muons are identified by requiring long tracks extending through more than 100 films with consistent alignment and minimal scattering relative to hadronic tracks. The muon momentum is measured using the multiple Coulomb scattering (MCS) technique, which analyzes the small angular deflections of the muon track as it traverses tungsten plates. These deflections arise from electromagnetic interactions with nuclei and are inversely proportional to the particle momentum. By measuring the scattering angles over the track length and applying the Highland formula, the momentum can be reconstructed with resolution $\Delta p/p \approx 0.30$ at 200 GeV. The method maintains good linearity up to several TeV, making it well-suited for the high-energy neutrino spectrum at FASER. The muon track topology, characterized by its length, straightness, and minimal energy deposition, provides clear separation from electromagnetic showers and hadronic tracks.

This represents the first measurement of ν_μ charged-current cross sections above 350 GeV. The measurement agrees well with Standard Model predictions and complements measurements from accelerator neutrino experiments (MINOS, NOMAD) and atmospheric neutrino experiments (IceCube).

4.3 Energy-Dependent Measurements

Another measurements using the FASER electronic detector with 65.6 fb^{-1} provide differential cross-section measurements as a function of neutrino energy. The electronic detector, equipped with a 0.57 T magnetic spectrometer and silicon tracking stations, enables precise momentum and charge measurements of muons produced in ν_μ and $\bar{\nu}_\mu$ charged-current interactions. Unlike the emulsion detector which requires offline microscopic analysis, the electronic detector provides real-time triggering capabilities and rapid event reconstruction, allowing analysis of much larger datasets.

The measurements use muons that exit the emulsion detector and traverse the spectrometer, where the magnetic field bends their trajectories according to their charge and momentum. Track reconstruction in the silicon layers determines the curvature, providing momentum measurement with resolution better than 30% for muons above 200 GeV. The charge sign identification capability is crucial for separating neutrino from anti-neutrino interactions. The neutrino energy is inferred from the measured muon momentum combined with the predicted flux spectrum and kinematic constraints from deep inelastic scattering.

These measurements separate ν_μ, $\bar{\nu}_\mu$, and combined $\nu_\mu + \bar{\nu}_\mu$ contributions across three energy bins (100-300 GeV, 300-600 GeV, 600-1000 GeV) plus a high-energy bin (> 1000 GeV). The ability to distinguish neutrinos from anti-neutrinos enables studies of isospin structure functions and provides sensitivity to parton distribution function asymmetries.

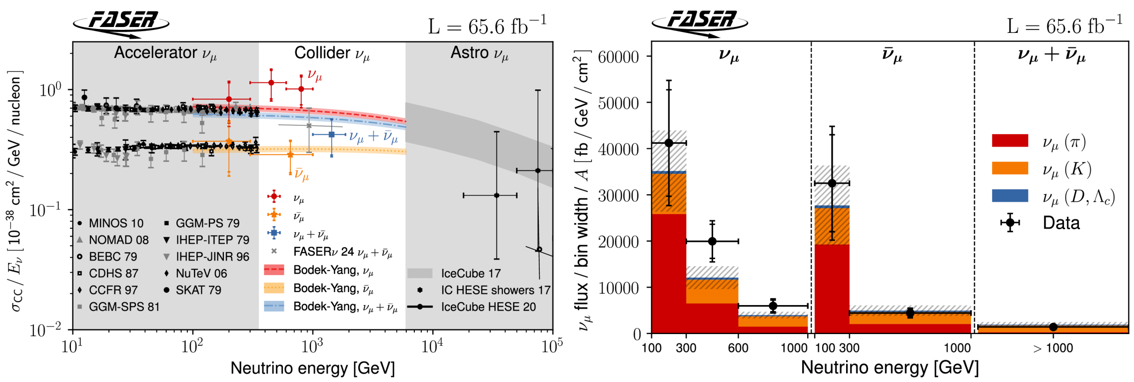

Figure 3: (Left) Measured CC neutrino-nucleon cross sections divided by neutrino energy as a function of neutrino energy (colored markers), compared to predictions from the Bodek-Yang model (colored lines) and previous measurements from fixed-target and astrophysical sources (gray/black markers). The horizontal error bars show the widths of the energy bins. The common high-energy bin contains neutrinos and anti-neutrinos with a momentum larger than qty1TeV. This corresponds to the flux-weighted average cross section. It has a width of qty868.2GeV which contains 68.3% of the simulated events. (Right) The measured neutrino flux divided by the energy and the cross sectional area of the fiducial volume (black markers) is compared to the expectation from the simulation (histograms). The inner error bars show the statistical uncertainty and the outer error bars the total uncertainty. The hatched area indicates the systematic uncertainties.

The results demonstrate good agreement with Bodek-Yang model predictions across all energy bins, providing the first direct measurements in the collider neutrino energy regime with consistency to the approximately linear energy dependence expected from deep inelastic scattering.

5. Summary and Outlook

FASER has achieved several groundbreaking results in neutrino physics including the first observation of neutrinos at a particle collider, the first detection of ν_e and ν_μ at the LHC, the first neutrino cross-section measurements in the TeV energy range, and the highest energy neutrino with flavor identification (E_e = 1.5 TeV).

The full LHC Run 3 dataset (expected ~250 fb^{-1}) will provide approximately 200 times more events, enabling precision measurements of energy-dependent cross sections, separation of neutrino and anti-neutrino contributions, constraints on parton distribution functions at high-x and low-Q^2, searches for beyond-Standard-Model physics in neutrino interactions, and first measurements of ν_τ cross sections at TeV energies.

FASER will continue operations through LHC Run 4. Looking further ahead, the proposed Forward Physics Facility would host upgraded detectors (FASER2 and FASERν2) during the High-Luminosity LHC era, targeting approximately one million high-energy neutrino interactions and opening new frontiers in forward physics [7].

Acknowledgments

FASER is supported by the Heising-Simons Foundation, Simons Foundation, CERN, ERC (KAKENHI), NSF, and the Swiss National Science Foundation. We thank the LHC for excellent performance, the ATLAS Collaboration for luminosity information and spare modules, and CERN for outstanding support.

References

[1] A. Ariga *et al.* [FASER], "FASER: ForwArd Search ExpeRiment at the LHC," arXiv:1811.10243 [physics.ins-det].

[2] H. Abreu *et al.* [FASER], "The FASERν detector," JINST **19**, P05066 (2024), arXiv:2504.13008 [physics.ins-det].

[3] R. Aben *et al.* [FASER], "Detecting and studying high-energy collider neutrinos with FASER at the LHC," Eur. Phys. J. C **83**, 241 (2023), arXiv:2207.00413.

[4] H. Abreu *et al.* [FASER], "First Direct Observation of Collider Neutrinos with FASER at the LHC," Phys. Rev. Lett. **131**, 031801 (2023), arXiv:2303.14185.

[5] FASER Collaboration, "First Measurement of the ν_e and ν_μ Interaction Cross Sections at the LHC with FASER's Emulsion Detector," Phys. Rev. Lett. **133**, 021802 (2024), arXiv:2403.12520.

[6] FASER Collaboration, "Updated ν_e and ν_μ Charged-Current Cross Section Measurements with the FASERν Emulsion Detector," CERN-FASER-CONF-2025-002 (2025).

[7] J. L. Feng *et al.*, "The Forward Physics Facility: Sites, Experiments, and Physics Potential," arXiv:2503.19010 [hep-ph].